$(\vec{t},p)$ reaction on ^{56}Fe, ^{58,60,64}Ni: Structure and reaction-mechanism effects

W. P. Alford
Department of Physics, University of Western Ontario, London, Ontario, Canada

R. N. Boyd and E. Sugarbaker
Nuclear Structure Research Labcratory, University of Rochester, Rochester, New York 14627

D. L. Hanson and E. R. Flynn
Los Alamos Scientific Laboratory, Los Alamos, New Mexico 87545

(Received 26 June 1979)

Differential cross sections and analyzing powers have been measured for the $(\vec{t},p)$ reaction on ^{56}Fe, ^{58,60,64}Ni at an incident energy of 17 MeV. Data were obtained for states up to an excitation of 3.7, 3.13, 2.8, and 4.9 MeV in ^{58}Fe, ^{60,62,66}Ni, respectively, including about ten states each with spin and parity 0^+, 2^+, and 4^+, and two states each with 3^- and 5^-. The measured analyzing powers show angular distributions characteristic of the L transfer, with variations from state to state comparable to those observed for cross sections of a given L. Angular distributions of the differential cross sections for strong transitions were generally fitted well by a standard distorted-wave Born approximation calculation. There appear to be significant discrepancies between the data and distorted-wave Born approximation predictions for excited 0^+ states and for most 4^+ states. Distorted-wave Born approximation predictions of analyzing power were in qualitative agreement with the data for ground-state transitions and for strong $L=2$ transitions but this was not true for $L=0$ transitions to excited states and for transitions with $L>2$. The effect of varying the optical parameters used in the distorted-wave Born approximation calculations was investigated; it was found that predictions of analyzing power for $L>0$ were quite sensitive to the choice of proton potential. The effects of two-step reaction processes were also investigated. These were found to produce large changes in predicted cross sections and analyzing powers, which could account for some of the discrepancies between these results and distorted-wave Born approximation predictions.

[NUCLEAR REACTIONS ^{56}Fe, ^{58,60,64}Ni$(\vec{t},p)$ $E=17$ MeV; polarized beam; enriched targets; measured $\sigma(E_p,\theta)$, $A_y(E_p,\theta)$; DWBA; coupled reaction channel analysis.]

I. INTRODUCTION

The study of particle transfer reactions has provided much of the information leading to our present understanding of certain aspects of nuclear structure. The most elementary of such reactions, single-particle transfer, has been widely studied, and the theoretical framework necessary for analysis of such data has been extensively developed. Two-nucleon transfer reactions have received less attention, but considerable experimental and theoretical effort has been devoted to their study. The results have yielded much spectroscopic and nuclear structure information, particularly relating to the effects of pairing forces in the nuclear interaction.[1]

Interpretations of two-nucleon transfer reactions have usually assumed that the two nucleons are transferred in a single step and in a relative singlet S state, and that a zero-range interaction between the transferred particles and the target can be used.[2] The adequacy of these assumptions has been tested in a number of investigations. Finite-range corrections[3-7] have been found to be important in accounting for the magnitude of measured cross sections, but do not produce much change in the shape of predicted angular distributions. However, transitions which are forbidden in the simple theory are observed, and measured cross sections have usually been accounted for by calculations assuming a two-step reaction mechanism.[8-14] Such calculations have shown that two-step contributions are probably important in allowed transitions as well. It is clearly important to understand these effects better, as two-nucleon transfer studies are used to investigate nuclear structure. The present analyzing power measurements were undertaken with this goal in mind.

Analyzing power measurements have been extensively pursued in single-particle transfer studies, but little data exist for two-nucleon transfer reactions.[15-20] A recent study[21] of the $(\vec{p},t)$ reaction on nuclei with strongly excited vibrational states indicates that the analyzing power measurements can provide a sensitive probe of the interplay between nuclear structure and reaction-mechanism effects.

The data presented in the present paper are

 © 1980 The American Physical Society

generally for strong natural parity transitions. The reaction analysis has been performed with a variety of procedures, including single-step distorted-wave Born approximation (DWBA), multistep processes involving inelastic excitation followed by direct two-nucleon transfer, and sequential neutron transfer. The standard DWBA calculations were fairly successful in representing the data for transitions to the strongly excited states, although some adjustment of the optical parameters was required to achieve this.

II. EXPERIMENTAL DETAILS

The present experiment utilized the polarized triton source[22] of the Los Alamos Scientific Laboratory (LASL) together with the FN model Van de Graaff accelerator. The incident beam energy was 17 MeV, the typical beam intensity on target was 50 nA, and the beam polarization (measured by the quench ratio method[23]) was typically 0.80.

The polarized triton beam was focused onto the enriched self-supporting metallic foil targets of ^{56}Fe, ^{58,60,64}Ni. The isotopic enrichment of the targets was $\geq 97\%$. Target thicknesses had been determined in an earlier experiment[24] by energy-loss measurements. Beam current in each run was measured in a Faraday cup with current integrator and was also monitored with a solid-state counter located at a scattering angle of 30° in the scattering chamber.

The reaction protons were momentum analyzed with the LASL quadrupole-dipole-dipole-dipole (QDDD) magnetic spectrometer and detected with the 1 m long helical wire focal plane detector.[25] Signals representing position (x), particle energy loss in the counter gas (ΔE), and energy loss in the detector scintillator (E) were processed by an on-line computer system. Particle identification was accomplished by two-dimensional gates (in x and E) placed on the E signals. A typical position spectrum for the resulting protons, that for ^{58}Ni(t,p), is shown in Fig. 1. The overall resolution achieved, about 40 keV full width at half maximum (FWHM), was almost completely due to the large target thicknesses.

Data were event recorded on magnetic tape, and played back for final off-line analysis. Several of the observed peaks were, for several angles, observed to be superimposed on background contaminant peaks. For such cases, the background was fitted and subtracted from the peak sums. The contaminated peaks were principally C and 0 on the target.

Data were taken for an angular range of 10° to 60° (lab). The data for the ^{56}Fe and ^{58}Ni targets were taken in conjunction with a $(\vec{t},p)$ study[14] to

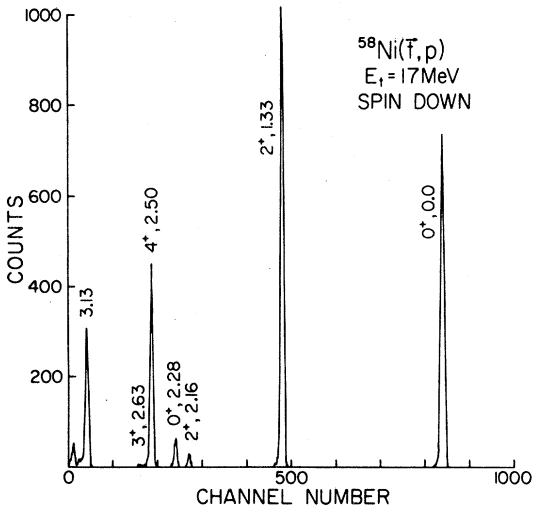

FIG. 1. Typical spectrum obtained with ^{58}Ni target.

(weakly excited) unnatural parity states, so the statistical uncertainties for the strongly excited states in ^{58}Fe and ^{60}Ni are particularly small. Only one magnetic field setting of the QDDD spectrometer was used for the ^{56}Fe and ^{58,60}Ni targets, but two were used for the ^{64}Ni target. Thus ^{66}Ni states were observed to considerably higher excitation energies than were states in ^{58}Fe or ^{60,62}Ni.

For the targets of ^{56}Fe, ^{58}Ni, and ^{60}Ni, angular distributions were recorded for transitions to most known levels up to the maximum energy observed. The energy resolution was adequate to permit clear identification of each group. For the ^{64}Ni target, groups were identified by comparison with the (t,p) results of Darcey *et al.*,[26] and excitation energies reported here are taken from that work.

III. EXPERIMENTAL RESULTS

At each angle, data were taken in two runs, one with spin down and one with spin up. The differential cross sections for these cases are given by

$$\frac{d\sigma}{d\Omega}(\theta)\Big|_{\pm} = \frac{d\sigma}{d\Omega}(\theta)\Big|_{0} [1 \pm p_{\pm} A_y(\theta)],$$

where $d\sigma/d\Omega$ is the differential cross section with an unpolarized incident beam and p_+ and p_- represent the beam polarization in the spin down and spin up runs, respectively. The cross sections and analyzing powers for comparison with theoretical calculations were obtained as

$$\frac{d\sigma}{d\Omega}\Big|_{0} = \frac{P_- \frac{d\sigma}{d\Omega}\Big|_{+} + p_+ \frac{d\sigma}{d\Omega}\Big|_{-}}{p_+ + p_-}$$

and

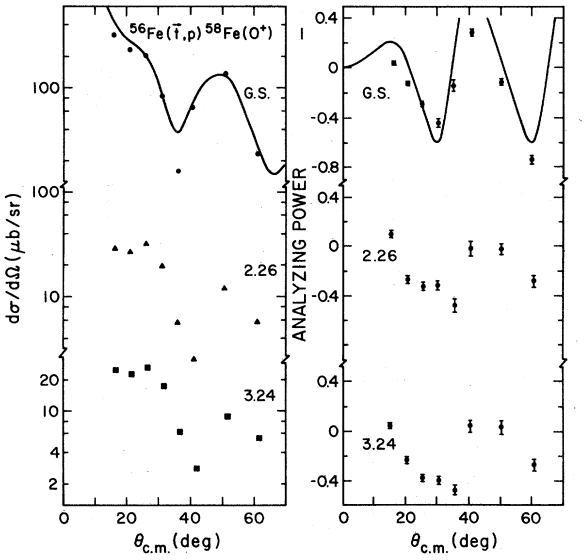

FIG. 2. Angular distributions for $L=0$ transitions with ^{56}Fe target. The curves are the result of DWBA calculations with a $(p_{3/2})^2$ form factor as described in the text, averaged over the angular acceptance of the spectrometer. The calculated cross section is normalized to the data, yielding an enhancement factor given in Table II.

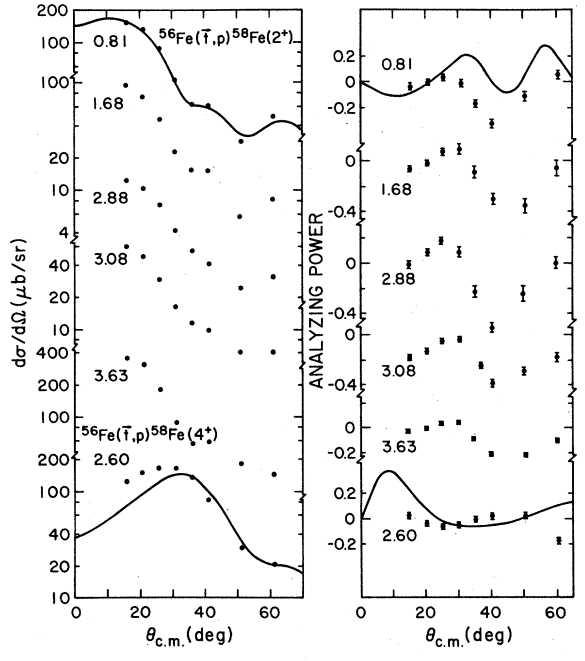

FIG. 3. Angular distributions for $L=2$ and $L=4$ transitions with ^{56}Fe target. The curves are the result of DWBA calculations with $(p_{3/2})^2$ form factor for $L=2$ and $(f_{5/2})^2$ for $L=4$.

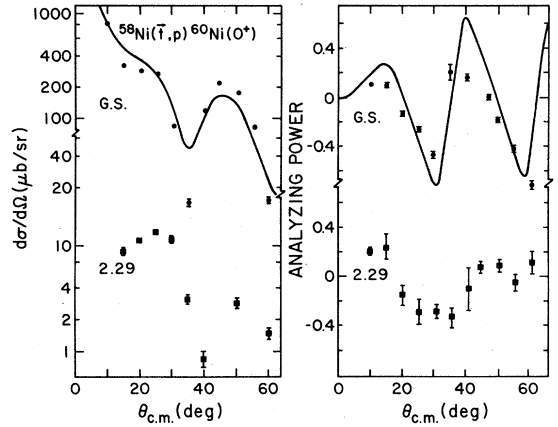

FIG. 4. Angular distributions for $L=0$ transitions with ^{58}Ni target. The curves have the same significance as in Fig. 2.

$$A_y(\theta)=\frac{\left.\frac{d\sigma}{d\Omega}\right|_+-\left.\frac{d\sigma}{d\Omega}\right|_-}{(p_++p_-)\left.\frac{d\sigma}{d\Omega}\right|_0}.$$

Angular distributions of cross section and analyzing power are presented in Figs. 2 through 12 for each target studied. Error bars shown on the data points are due to statistical uncertainties only. For many of the cross sections, these were smaller than the size of the data points. The curves are the result of DWBA calculations to be described later.

The cross section distributions show a shape generally characteristic of the L transfer, with some variation for transitions to different levels of the same spin and parity, a result well known in such measurements. It also appears that the analyzing power distributions are characteristic of the L transfer with small variations from level to level. This result may be inferred from earlier

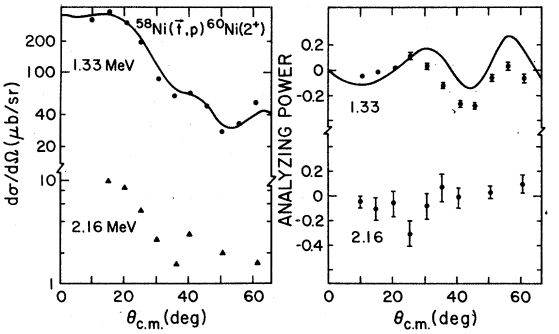

FIG. 5. Angular distributions of $L=2$ transitions for ^{58}Ni target. The curves have the same significance as in Fig. 3.

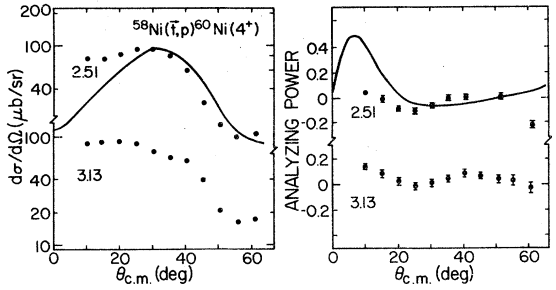

FIG. 6. Angular distributions of $L=4$ transitions for ^{58}Ni target. The curves have the same significance as in Fig. 3.

measurements,[20] but the present results provide much more data to support this conclusion. For $L=0$ transitions the analyzing power exhibits dramatic oscillations, even though the large angular acceptance of the spectrograph ($\pm 3.4°$) provides significant averaging of this very sharp angular structure. The magnitude of the analyzing power is approximately proportional to the angular derivative of the cross section, similar to the behavior observed in the elastic scattering of polarized protons at low energy.

^{56}Fe(t,p)^{58}Fe

The differential cross section and analyzing power data for this reaction to 0^+ levels in ^{58}Fe are presented in Fig. 2, and those to 2^+ and 4^+ levels in Fig. 3. Complete angular distributions were obtained for all the levels listed in the tabulations below an excitation of 3.7 MeV, except for the 4^+ level at 2.077 MeV, a level of unknown spin at 3.133 MeV, and the 2^+ level at 3.233 MeV. The

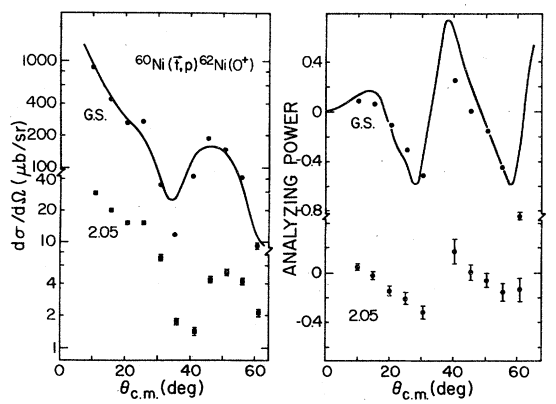

FIG. 7. Angular distributions of $L=0$ transitions for ^{60}Ni target. The curves have the same significance as in Fig. 2.

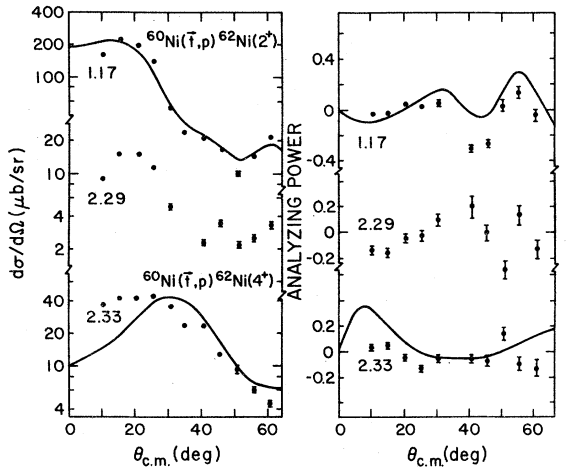

FIG. 8. Angular distributions of $L=2$ and $L=4$ transitions for ^{60}Ni target. The curves have the same significance as in Fig. 3.

data for the unnatural parity states at 2.133 (3^+), 2.782 (1^+), and 3.537 MeV (1^+) were presented in an earlier publication.[14] The 2^+ state at 3.233 MeV was not resolved from the 3.243 MeV level in the present experiment. However, the previous higher resolution (t,p) work at 12 MeV suggests that only the 0^+ level is excited appreciably. This is supported by the great similarity between the angular distributions to the levels at 2.26 and 3.24

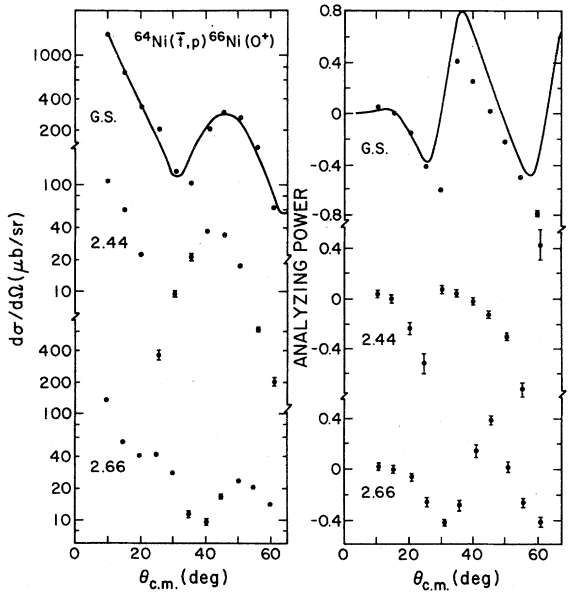

FIG. 9. Angular distributions for $L=0$ transitions for ^{64}Ni target. The solid curves have the same significance as in Fig. 2.

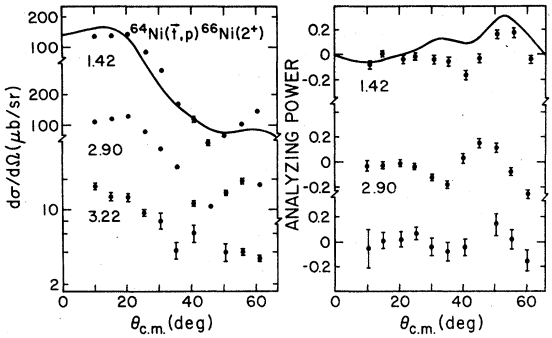

FIG. 10. Angular distributions for $L=2$ transitions for ^{64}Ni target. The curves have the same significance as in Fig. 3.

MeV.

Noteworthy for the ^{56}Fe(t,p) data are the differential cross section and analyzing power angular distributions for the 2^+ levels: for all five levels the shapes of both are very nearly identical, even though the magnitudes of the peak cross sections differ by more than an order of magnitude. The differences in the angular distributions are more pronounced for the 0^+ levels: the minima for the cross sections to the 2.26 and 3.24 MeV levels appear to be around 42°, while that for the ground state is around 35°. That shift is also reflected in the analyzing powers for the levels.

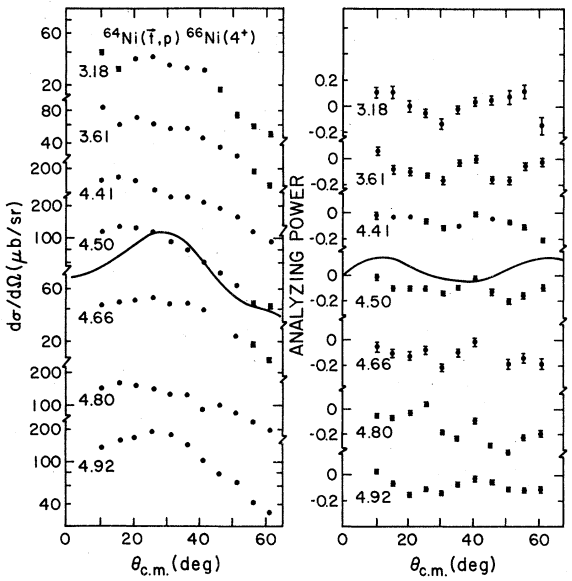

FIG. 11. Angular distributions for $L=4$ transitions for ^{64}Ni target. The curves have the same significance as in Fig. 3.

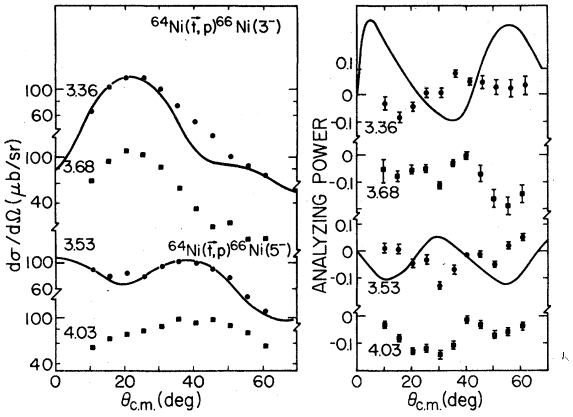

FIG. 12. Angular distributions for $L=3$ and $L=5$ transitions for ^{64}Ni target. The curves were calculated with a $(g_{9/2}f_{5/2})$ form factor. The calculated cross section is normalized to the data, yielding enhancement factors given in Table II.

^{58}Ni$(t,p)^{60}$Ni

The differential cross sections and analyzing powers for levels in ^{60}Ni below 3 MeV excitation are shown for 0^+, 2^+, and 4^+ levels in Figs. 4, 5, and 6, respectively. Data for the ^{60}Ni (3^+, 2.626 MeV) level were published previously.[14] In addition, the 4^+, 3.130 MeV level is reported: it could have contributions from several nearby levels, but the 12 MeV ^{58}Ni(t,p) data[26] suggests that it dominates over those states in the (t,p) reaction.

The 0^+ levels exhibit the same qualitative behavior as they do in ^{58}Fe: the angular distributions to the ground state and excited states are most notably different in the location of the differential cross section minimum at around 40°, and the features of the analyzing power are less dramatic in the excited-state angular distribution than they are for that of the ground state. Some differences are seen in the differential cross sections to the 2^+ levels, and those differences are enhanced in the analyzing powers. Finally, the angular distributions for the two 4^+ levels are quite similar, both in cross section and analyzing power.

^{60}Ni$(t,p)^{62}$Ni

Data for this reaction are shown in Figs. 7 and 8 for (t,p) to 0^+ states and to 2^+ and 4^+ states, respectively. The states for which data are shown represent the known levels below 2.8 MeV of excitation.

The angular distributions for the 0^+ and 2^+ levels have qualitative features very similar to those for the ^{58}Ni(t,p) reaction. The differences between angular distributions for the ground state and ex-

cited 0^+ level are not as pronounced as for the lighter isotope, however, as the minimum in the differential cross section is shifted by less than 5° between the two. The analyzing powers also show more similarity than for ^{58}Fe and ^{60}Ni. The angular distributions to the 2^+ levels show some differences, notably in the analyzing powers at around 40° where they are actually out of phase. The angular distribution to the 4^+ level is very similar to those for the 4^+ levels in ^{58}Fe and ^{60}Ni.

^{64}Ni(t,p)^{66}Ni

The data for this reaction are presented in Figs. 9 ($L=0$ transfers), 10 ($L=2$ transfers), 11 ($L=4$ transfers), and 12 ($L=3$ and $L=5$ transfers). Transitions were observed to all reported levels up to 3.70 MeV, although that to the 2.965 MeV level was very weak. Between 3.70 and 4.95 MeV, transitions were not observed to levels reported at 3.716, 3.746, 3.782, 4.057, 4.078, 4.125, 4.696, and 4.738 MeV. From the results of Darcey *et al.*[26] those at 3.746, 3.782, and 4.125 MeV might have been expected to appear with appreciable intensity, but the others were reported as weakly excited. A group was also seen close to the expected location for the 4.028 MeV level, but it appears to be due to an impurity. There was no indication from the results of Darcey *et al.* that any of the groups should involve unresolved levels.

Three 0^+ levels in ^{66}Ni are seen. As with the nuclei discussed above, the differential cross section of the first excited 0^+ level (at 2.44 MeV) has its first minimum shifted from that of the ground state. However, it is shifted in the opposite direction from the excited-state minima in the lighter nuclei. The second excited state (at 2.66 MeV) has its minimum in that region (40°) shifted in the same direction as for the excited 0^+ states in the other nuclei. The analyzing powers are characteristic of $L=0$ transfers, thus confirming these spin assignments.

Three levels thought to be 2^+ states are populated with appreciable strength. The first two, at 1.42 and 2.90 MeV, are similar in their angular distributions, although the analyzing powers are shifted somewhat at back angles. The third state, at 3.22 MeV, is quite weakly excited, but it has an angular distribution nearly identical to that of the second 2^+. The analyzing powers of the three levels are qualitatively similar, and exhibit the back angle rise which seems to be characteristic of $L=2$ transfers.

Seven levels are nominally classified as being populated by $L=4$ transfers. The differential cross sections for all of these levels are rather featureless, exhibiting a slow back angle falloff from a forward angle plateau. The analyzing powers show a fairly consistent behavior for the forward angles, but differ considerably at back angles. Note that the 3.179 MeV level could well have some contribution to it from the 3.219 MeV level, tentatively assigned 2^+ from the previous (t,p) work.[26] This might explain the positive analyzing power at large angles seen for the 3.179 MeV level in the present experiment.

Four fairly strongly excited states were seen which were clearly excited by an L transfer greater than 2 and did not have the features of the $L=4$ transfers discussed above. Two of these appear, from the differential cross sections, to have $L=3$, as was concluded in the previous (t,p) work, and the other two to have $L=5$. The analyzing powers are small for all four levels, but are similar in their forward angle behavior for each pair of states having the same L transfer.

IV. REACTION CALCULATIONS

A number of distorted-wave Born approximation (DWBA) and multistep reaction calculations were performed in an effort to understand the differences observed in the angular distributions for transitions of a given L transfer. Particular attention was focused on the $L=0$ transitions, since these showed the most characteristic structure both in differential cross sections and analyzing power.

A. DWBA calculations

As a starting point, optical parameters were taken from analyses of the elastic scattering of protons[27,28] and tritons[29] at 15 MeV. A spin-orbit potential of magnitude 6 MeV as used in Ref. 20 was added to the triton potential. Calculations for the (t,p) reaction leading to the ground state of ^{62}Ni were carried out using these, and slight adjustments were made in the proton potentials as described below. The potentials finally used are listed in Table I. The calculation was done with the code DWUCK4[30] with spin-orbit potentials included in both scattering channels and in the bound state. A zero-range interaction and local potentials were used in all calculations. A variety of form factors was used, involving the $p_{1/2}$, $p_{3/2}$, $f_{5/2}$, and $g_{9/2}$ orbits. The first three orbits are known to be most important in this region, but the $g_{9/2}$ single-particle state is identified at low excitation, and pickup measurements[31] show a significant $(g_{9/2})^2$ component in the ground state of ^{64}Ni.

Using either proton potential it is possible to achieve reasonable fits to both the cross section and analyzing power for ground-state transitions. The predicted angular dependence of both cross

TABLE I. Optical parameters used in reaction calculations.

	$-V$ (MeV)	r_0 (fm)	a_0 (fm)	$-W$ (MeV)	r_I (fm)	a_I (fm)	$-W_D$ (MeV)	$-V_{so}$ (MeV)	r_{so} (fm)	a_{so} (fm)
t [a]	169.7	1.16	0.732	22.8	1.5	0.796	0.0	6.0	1.16	0.758
$P1$ [b]	$61.8-0.32Z$ $+24(N-Z)/E$ $+0.4Z/A^{1/3}$	1.12	0.78	0.0	1.32	0.59	$11.2-0.25E$ $+12(N-Z)/A$	6.2	1.01	0.75
$P2$ [c]	$58.3-0.55E$ $+27(N-Z)/A$ $+0.4Z/A^{1/3}$	1.25	0.65	0.0	1.25	0.47	13.5	7.5	1.25	0.47

[a] Reference 29 with V_{so} from Ref. 20.
[b] Reference 27 with modification of V, W, W_D.
[c] Reference 28 with modification of V.

section and analyzing power was found to be very similar for $(p_{1/2})^2$, $(p_{3/2})^2$, or $(f_{5/2})^2$ form factors. The predictions were somewhat different for a $(g_{9/2})^2$ form factor, particularly for A_y, but a $(g_{9/2})^2$ component of plausible magnitude in a mixed form factor had little effect on predictions for the ground-state transitions. The dependence on form factor for $L=0$ transitions is illustrated in Fig. 13. In the light of these results, a series of calculations was carried out with a simple $(p_{3/2})^2$ form factor to investigate the sensitivity of the predictions to the choice of optical parameters.

The predictions were insensitive to small changes in the triton well parameters, so that these were held fixed at the values given in Table I. In order to fit the location of the first minimum in the $L=0$ cross section, it was necessary to increase the depth of the real-central term in the proton potential. An increase of 3 MeV was required for the set from Ref. 27 (set $P1$) and 5 MeV for that from Ref. 28 (set $P2$). In addition, in order to fit the forward angle data, it was necessary to set the volume imaginary potential equal to zero and reduce the surface absorption potential by about 10% for the set from Ref. 27.

For transitions with $L=2$, it was found that calculations with proton parameter set $P2$ provided better fits to both the angular distributions and analyzing powers than those of $P1$. As a result, the former set was chosen for the further analysis of the data, and all curves shown in Figs. 2–12 were calculated with proton parameter set $P2$. It should be noted, however, that either proton potential resulted in similar predictions for the other L values observed here, $L=0$, 3, 4, and 5.

A comparison of the results of calculations using the proton potentials $P1$ and $P2$ suggested that the predicted analyzing powers for $L=2$ transitions were particularly sensitive to the radius of the proton spin-orbit potential. The effect of changing this parameter is shown in Fig. 14, and it is seen that large changes in A_y may be pro-

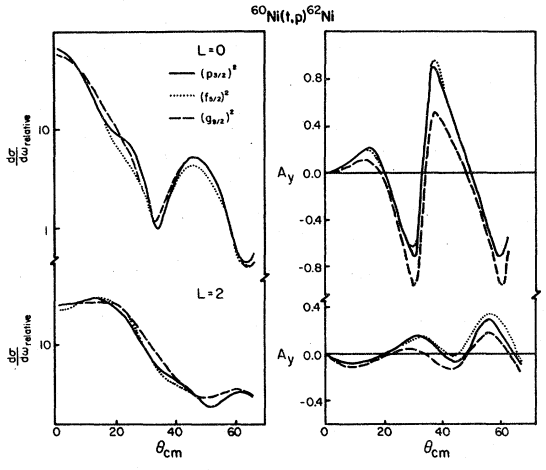

FIG. 13. Dependence of DWBA calculations on form factor of transferred particles. For $L=2$ transfer the results for $(p_{1/2}p_{3/2})$, $(p_{3/2}f_{5/2})$, and $(p_{1/2}f_{5/2})$ are identical with those for $(p_{3/2})^2$.

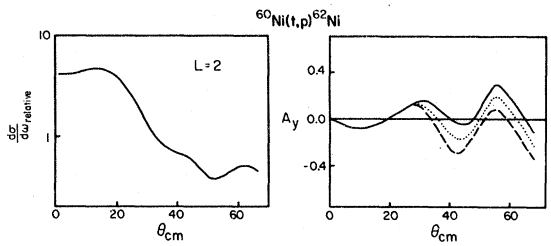

FIG. 14. Dependence of DWBA results on radius of proton spin-orbit potential for $r_{so}=1.25$ (solid), 1.20 (dotted), and 1.15 (dashed) fm. The cross section is unaffacted by the changes in r_{so} shown.

duced with no significant change in the predicted cross section. It must be noted, however, that such changes in the spin-orbit potential result in unacceptably large changes in the predicted analyzing powers for elastic scattering. As a result, all DWBA calculations were carried out with spin-orbit potentials derived from elastic scattering measurements as given in Refs. 27 and 28.

For the $L=0$ transitions the DWBA predictions have been averaged over an angular range equivalent to the entrance aperture of the spectrograph for comparison with the data. For transitions with $L>0$, the angle averaging did not produce appreciable changes in the calculated cross sections or analyzing powers.

For all ground-state transitions the DWBA calculations provide reasonable agreement with the cross section data, although the detailed fit is not very good for the ^{58}Ni target. For $L=0$ transitions, the analyzing power is generally proportional to the derivative of the angular distribution of cross section. As long as the cross section is fitted by the calculations, the qualitative features of the analyzing power distributions are reproduced. In many cases extreme values of A_y are in substantial disagreement with the calculations, and the detailed fit to the data is not very satisfactory.

The data for all $L=0$ transitions to excited states show the position of the first minimum displaced relative to that of the ground-state transition, with the shift much larger than predicted by the Q dependence of the DWBA calculations. The representation of both the cross section and analyzing power data for the ^{66}Ni (0^+, 2.44 MeV) state can be improved by assuming that the form factor for this transition is dominated by a $(g_{9/2})^2$ component. This results in a shift of the first minimum in the cross section toward forward angles. All other $L=0$ transitions to excited states had the first minimum in the cross section shifted to a larger angle than did the ground-state transitions. This shift could not be reproduced by DWBA calculations with the optical parameters held fixed and the form factor constructed with combinations of $(p_{1/2})^2$, $(p_{3/2})^2$, $(f_{5/2})^2$, and $(g_{9/2})^2$ components. The analyzing power data for these transitions were qualitatively similar to the results for ground-state transitions, although the range of variation was generally reduced.

The DWBA predictions for $L=2$ transitions with a $(p_{3/2})^2$ form factor are shown as the solid curves in Figs. 3, 5, 8, and 10. Other form factors involving (fp) orbits [$(p_{1/2},p_{3/2})$, $(f_{5/2},p_{3/2})$, and $(f_{5/2},p_{1/2})$] all gave predictions indistinguishable in shape from that for the $(p_{3/2})^2$ form factor, but with a simple scaling in magnitude. For $(f_{5/2})^2$ or $(g_{9/2})^2$ form factors, the DWBA predictions were similar in shape and provided adequate fits to the cross section data.

The angular variation of the analyzing power data is quite similar for all strong $L=2$ transitions, with a sizable negative value between 35° and 40°, followed by an increase, usually to positive values, at larger angles. The qualitative features of this behavior were reproduced by the calculations, but as with the ground-state transitions, the actual magnitudes of the measured analyzing powers often showed substantial disagreement with calculations.

In contrast with cross sections, predicted analyzing powers showed significant dependence on the form factor used in the calculations. This is illustrated in Fig. 13 which shows calculated cross sections and analyzing powers for both $L=0$ and $L=2$ transitions for a variety of reasonable form factors. In the light of this result, it might be expected that better fits would be obtained with mixed form factors derived from "realistic" shell model calculations for the states of interest. No such calculations which included particles in the $g_{9/2}$ orbit were available, although the experimental data point to the importance of this state in most of the nuclei of interest at low excitation energies.[31] Since the DWBA predictions are sensitive to $(g_{9/2})^2$ components in the form factor, it was concluded that little more could be learned by using complex wave functions which did not include particles in this shell model state.

For $L=4$ transitions, calculations were carried out assuming $(f_{5/2})^2$ for the form factor, and the results are shown in Figs. 3, 6, 8, and 11. The predictions were almost identical, except for the magnitude of the cross section, for $(g_{9/2})^2$ form factor. The calculations characteristically show poor agreement with both cross sections and analyzing power data at forward angles.

Four transitions to negative parity states were identified in ^{66}Ni. The shapes of the cross section distributions are fitted well with simple $(f_{5/2}g_{9/2})$ or $(p_{3/2}g_{9/2})$ form factors. The asymmetries are small but significantly different from zero, and are not fitted well by the DWBA calculations.

B. Multistep reaction calculations

The success of the DWBA in representing simple, e.g., single-nucleon stripping or pickup, reactions has confirmed its basic accuracy. However, its straightforward application to two-nucleon stripping does not produce the same level of agreement between theory and experiment. For example, in the present study, the proton optical potential parameters required some modification

to represent the (t,p) transitions to ground states. While this has been found to be necessary in many two-nucleon transfer reaction studies, such parameter modifications were not necessary to represent single-nucleon transfer data. Furthermore, the excited 0^+ levels generally exhibit angular distributions quite different from those to the ground state, both in differential cross sections and analyzing powers.

It was therefore decided to perform a qualitative investigation of possible contributions of multistep reaction processes to the (t,p) differential cross sections. Both coupled channel Born approximation (CCBA) calculations, in which reaction trajectories including inelastic excitations are taken into account, and consecutive reaction channel (CRC) calculations, in which sequential transfer mechanisms are included, were examined. It was immediately concluded that the CCBA effects could contribute significantly only to weakly excited states. Since the difficulties described above are present even in the most strongly excited states, the focus of our attention was directed to the CRC calculations. The code CHUCK[30] was used to perform these calculations, and the triton potential and proton optical potential $P2$ given in Table II were used. The reaction steps assumed were (t,d,p). The spin 1 deuteron state was assumed; the deuteron channel was described with the optical potential parameters (with $r_0 = 1.1$ fm) of Childs *et al.*[32]

The results of a calculation in which only sequential transfer is included in a $0^+ \rightarrow 0^+$ calculation are compared to those of a standard (as described above) one-step two-nucleon transfer calculation in Fig. 15. The transfer assumed for both calculations was $(p_{3/2})^2$. Two effects are immediately apparent from that figure: (1) The major minimum at around 30° is sharply shifted forward, and (2) the magnitude of the cross section for the CRC calculation is considerably smaller than that for the one-step calculation. Since the enhancement factor needed to scale the predicted cross section to those observed for the strongest transitions is close to 1.0 (assuming the usual zero-range scaling factor), the CRC results are apparently not capable of yielding a sufficiently large cross section for those states. However, this generally applies only to the ground-state transitions; all others could well have appreciable mixtures of one- and two-step transfers. The significant differences in the shapes of the ground- and excited-state angular distributions suggest that the mechanisms included in their population are indeed different.

The results of two calculations in which one- and two-step transfers were mixed are shown in Fig. 16. In those calculations the transition strengths (zero-range scaling factors) were multiplied by a normalizing factor α which could be varied in the calculations. The normal full

TABLE II. (t,p) enhancement factors, ϵ.

	E_x (MeV)	L^π	Form factor	
^{56}Fe → ^{58}Fe	0.0	0^+	$(p_{3/2})^2$	0.87
	2.26	0^+	$(p_{1/2})^2$	0.31 [a]
	0.81	2^+	$(p_{3/2})^2$	0.23
	2.59	4^+	$(f_{5/2})^2$	5.70
^{58}Ni → ^{60}Ni	0.0	0^+	$(p_{3/2})^2$	1.15
	2.29 [a]	0^+		
	1.33	2^+	$(p_{3/2})^2$	0.65
	2.51	4^+	$(f_{5/2})^2$	5.20
^{60}Ni → ^{62}Ni	0.0	0^+	$(p_{3/2})^2$	0.97
			$(f_{5/2})^2$	18.0
			$(g_{9/2})^2$	8.9
			$(p_{1/2})^2$	2.0
	1.17	2^+	$(p_{3/2})^2$	0.34
			$(f_{5/2})^2$	7.7
			$(g_{9/2})^2$	2.9
			$(f_{5/2}p_{1/2})$	0.77
			$(f_{5/2}p_{3/2})$	2.4
			$(p_{1/2}p_{3/2})$	0.2
	2.34	4^+	$(f_{5/2})^2$	4.8
			$(g_{9/2})^2$	2.0
^{64}Ni → ^{66}Ni	0.0	0^+	$(p_{3/2})^2$	2.2
	2.44	0^+	$(p_{1/2})^2$	0.33 [a]
	1.42	2^+	$(p_{3/2})^2$	0.23
	3.36	3^-	$(p_{3/2}g_{9/2})$	0.13 [b]
			$(f_{5/2}g_{9/2})$	5.3 [b]
	4.50	4^+	$(f_{5/2})^2$	3.3 [a]
	3.53	5^-	$(p_{3/2}g_{9/2})$	0.24 [b]
			$(f_{5/2}g_{9/2})$	1.5 [b]

[a] Poor or no fit to σ and A_y.
[b] Good fit to σ, poor fit to A_y.

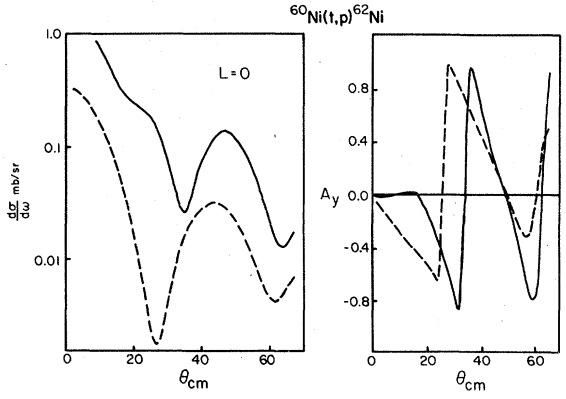

FIG. 15. Comparison of CRC calculations for pure one-step (solid) and pure sequential transfer (dashed) for $L = 0$. A $(p_{3/2})^2$ form factor was assumed.

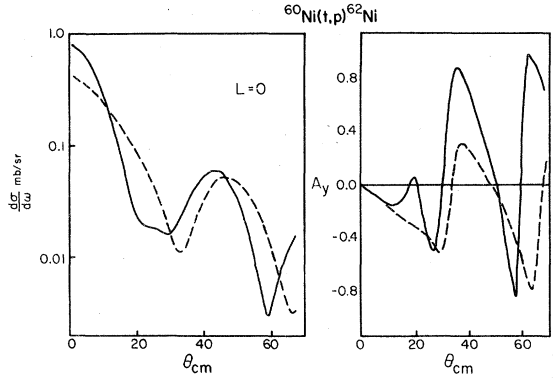

FIG. 16. Comparison of CRC calculations for one-step plus sequential transfer for $L=0$. Solid line, $\alpha_{tp}=-0.04$, dashed line, $\alpha_{tp}=+0.4$. A $(p_{3/2})^2$ form factor was assumed.

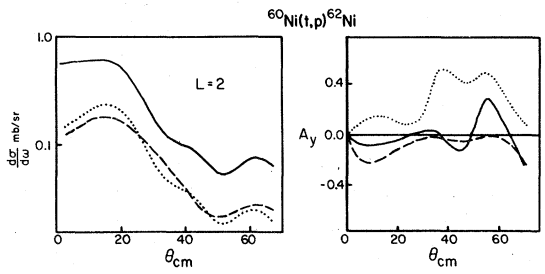

FIG. 17. Calculated cross sections for $L=2$ transfer assuming pure one-step and one-step plus sequential transfer. Solid line, one-step, $\alpha_{tp}=1.0$, dashed line, $\alpha_{tp}=-0.4$, dotted line, $\alpha_{tp}=+0.4$. A $(p_{3/2})^2$ form factor was assumed.

strengths were taken for the (t,d) and (d,p) reactions ($\alpha_{td}=\alpha_{dp}=1$), while the (t,p) factor was reduced, with $\alpha_{tp}=0.4$. Both relative phases between one-step and sequential transfer amplitudes were tried. It is seen that the straightforward application of the usual phases with $\alpha_{tp}=0.4$ produces a very interesting result. It has its cross section minimum at about the same location as was observed for the pure one-step calculation. But the amplitude of the analyzing power is considerably less than was seen in the one-step case, thus producing a significantly improved data representation for the excited 0^+ states. While the location of the predicted minimum for this one- plus two-step calculation is shifted toward small angles by about 5° from that seen in the data [see, e.g., the data for the ^{62}Ni (2.05 MeV) level], it should be recalled that the original motivation for increasing the proton real-central potential strength was to produce a 5° shift. Thus the use of *unmodified* parameters and about the mix of one- and two-step contributions used in the calculation with $\alpha_{tp}=0.4$ produces quite good agreement with the general features of the angular distributions for transitions to excited 0^+ levels. The use of the opposite phase ($\alpha_{tp}=-0.4$) produces a very strangely shaped cross section and an analyzing power with much too large an amplitude. Other calculations with this phase and different magnitudes of α_{tp} were tried; none produced as good a data representation as the one-step result.

Similar calculations were performed for (t,p) to the ^{62}Ni(2^+) levels. While the general features of the data are less dramatic than those for the $L=0$ transfers, significant differences in predictions between the various calculations are observed, as is seen in Fig. 17. Shown there are the predictions of a one-step calculation, and of two calculations in which the full sequential transfer strength is combined with some one-step ($\alpha_{tp}=\pm 0.4$) strength. As for the transfers to the 0^+ levels, all transfers in these calculations were assumed to involve $p_{3/2}$ orbits. The differential cross sections predicted by these calculations are seen to be very similar. However, the predicted analyzing powers show dramatic differences. The one- plus two-step calculation with the nonstandard phase ($\alpha_{tp}=-0.4$) produced a considerably better data representation than that with the standard phase. However, there is no appreciable improvement in data representation between the one-step calculation and the better of the one- plus two-step calculations. That the preferred phase for the 2^+ levels is the *opposite* of that preferred by the 0^+ levels merely accentuates the difficulties, together with the theoretical questions[9,12] with which this qualitative analysis did not attempt to deal, rendered the meaning of further analysis of this type questionable.

V. TRANSITION STRENGTHS

The preceding discussion has emphasized the comparison of the shapes of the measured and calculated angular distributions without regard to the magnitude of the cross section. Since this depends strongly on the form factor for the transition, a comparison of measured and calculated cross section magnitudes provides an indication of the validity of the assumed form factor. For some of the stronger transitions observed in these measurements, enhancement factors have been calculated as $\epsilon=\sigma_{expt}/\sigma_{DW}$. These are listed in Table II.

These results suggest that the $(p_{3/2})^2$ component is most important for the ground-state transition. For the lowest 2^+ states the $(p_{3/2})^2$ form factor seriously overestimates the cross section, while $(f_{5/2})^2$ or $(g_{9/2})^2$ form factors underestimate it, indicating that no simple form factor is adequate. For the strong transitions to 4^+ states the $(g_{9/2})^2$

component must be important. For the excited 0^+ states a $(g_{9/2})^2$ or $(f_{5/2})^2$ form factor would yield a reasonable enhancement factor, but the poor fit to the angular distribution indicates that the DWBA calculation is not providing a satisfactory model for the transition.

For the ground-state transitions, a more quantitative comparison may be made. Although the nickel isotopes lie near the closed shell at $N=Z=28$, it has been known for some time that the ground-state transition strengths show only qualitative agreement with pairing model predictions.[1] For the targets ^{58,60,64}Ni, the model would predict ground-state strengths in the ratio 1:1.5:2.5. These are to be compared with the enhancement factors 1.14:0.97:2.2 which are obtained on the assumption of a fixed form factor $(p_{3/2})^2$ for all transitions. The disagreement with model predictions indicates that the ground-state correlations are changing significantly as neutrons are added beyond $N=28$.

More realistic form factors for the ground-state transitions may be calculated using the results of Yoshida,[33] if the orbit occupancies $V(j)$ are known for the ground states. These can be obtained from a single-particle stripping and pickup data, though the results listed in the Nuclear Data Sheets show substantial inconsistencies for the heavier nickel isotopes. For the ^{58}Ni target, the data would imply a form factor $0.87(p_{3/2})^2+0.94(f_{5/2})^2+0.46(p_{1/2})^2+1.00(g_{9/2})^2$. This yields an enhancement factor of 0.80, which is quite reasonable. A similar result has been reported in a study of the ^{59}Ni(t,p)^{61}Ni reaction.[34] For the heavier isotopes, the experimental data are too uncertain to provide useful results.

The orbit occupancies can also be calculated in the BCS approximation[35] if the single-particle energies of the active orbitals are known. These may be obtained from the location of the states in ^{57}Ni, although it is clear that the $g_{9/2}$ orbit drops in excitation in the heavier isotopes of Ni.[36] A calculation was carried out using the single-particle energies shown in Table III, with the strength of the pairing interaction set at $G=0.33$ MeV. The single-particle energies appropriate for an even isotope of mass A were taken to be those for the odd isotope of mass $(A-1)$.

The resulting spectroscopic amplitudes $B_{jj}=(j+\frac{1}{2})^{1/2}U_i(j)V_f(j)$, where $U_i(j)$ is the vacancy in the initial state and $V_f(j)$ is the occupancy in the final state, are also shown in Table III. DWBA calculations using these amplitudes in the form factor yielded enhancement factors for the ground-state transitions as shown in Table IV. The variations in ϵ indicate that the BCS calculation does not fully account for variations in the observed cross sections, even though it does account for the change in single-particle energy for particles in the $g_{9/2}$ orbit.

VI. CONCLUSIONS

This study has provided a survey of cross section and analyzing power measurements for the (t,p) reaction. Data for a number of states with spin and parity 0^+, 2^+, and 4^+ show that the angular distribution of analyzing powers are generally characteristic of the L value in the reaction. Variations in A_y for transitions of a given L are observed to be analogous to the variations in cross section.

DWBA calculations are able to reproduce the main features of both the cross section and analyzing power, although detailed agreement is not really satisfactory for the analyzing power results. Calculations have shown that the predictions are sensitive to several factors, particularly for $L=2$ transitions. These include the particular optical-model parameter set chosen for the proton channel, the details of the proton spin-orbit potential, the form factor for the transferred particles, and possible sequential transfer contributions to the reaction mechanism.

Further measurements of this sort will be required if the relative importance of these different effects is to be assessed. It will be very desirable to obtain data for transitions for which

TABLE III. A list of single-particle energies, $\epsilon_j(A)$, in MeV as used in the BCS calculations of Sec. V. Here A is one unit less than the target mass. Also contained here are the spectroscopic amplitudes $B_{jj}(A)$, where A is now the target mass, as defined in Sec. V.

Orbit	$\epsilon_j(57)$	$B_{jj}(58)$	$\epsilon_j(59)$	$B_{jj}(60)$	$\epsilon_j(61)$	$B_{jj}(62)$	$\epsilon_j(63)$	$B_{jj}(64)$	$\epsilon_j(65)$
$p_{3/2}$	0.0	0.83	0.0	0.77	0.0	0.71	0.0	0.71	0.0
$f_{5/2}$	0.78	0.78	0.78	0.89	0.78	0.89	0.78	0.90	0.78
$p_{1/2}$	1.11	0.38	1.11	0.46	1.11	0.48	1.11	0.50	1.11
$g_{9/2}$	3.80	0.41	3.00	0.80	2.10	1.05	1.40	1.21	1.00

TABLE IV. Ground-state enhancement factors from BCS calculations.

Target	σ_{expt} (μb/sr) [a]	σ_{DW} (μb/sr) [a]	ϵ	$\epsilon_{Relative}$
^{58}Ni	155.0	245.0	0.63	1.00
^{60}Ni	160.0	310.0	0.52	0.83
^{64}Ni	280.0	400.0	0.70	1.11

[a] Experimental and DW cross sections taken at second maximum (~50°) of normalized and unnormalized distributions, respectively.

model calculations can provide realistic form factors.

ACKNOWLEDGMENT

This work was performed under the auspices of the U. S. Department of Energy. Support for one of the authors (W.P.A.) was through the NRESC of Canada, and we also acknowledge the support of the National Science Foundation (R.N.B. and E.S.).

[1]R. A. Broglia, O. Hansen, and C. Riedel, *Advances in Nuclear Physics*, edited by E. M. Baranger and E. Vogt (Plenum, New York, 1973), Vol. 6.
[2]I. S. Towner and J. C. Hardy, Adv. Phys. 18, 401 (1969) provides an extensive review of the standard formulation of the theory.
[3]P. D. Kunz and E. Rost, Nucl. Phys. A162, 376 (1971).
[4]B. F. Bayman and D. H. Feng, Nucl. Phys. A205, 513 (1973).
[5]C. L. Lin, S. Yamaji, and H. Yoshida, Nucl. Phys. A209, 135 (1973).
[6]T. Takemasa, Nucl. Phys. A220, 31 (1974).
[7]L. A. Charlton, Phys. Rev. C 12, 351 (1975).
[8]R. J. Ascuitto and N. K. Glendenning, Phys. Rev. C 2, 1260 (1970).
[9]D. K. Olsen, T. Udagawa, T. Tamura, and R. E. Brown, Phys. Rev. C 8, 609 (1973).
[10]N. B. deTakacsy, Nucl. Phys. A231, 243 (1974).
[11]M. J. Schneider, J. D. Burch, and P. D. Kunz, Phys. Lett. 63B, 129 (1976).
[12]V. Managoli, D. Robson, and L. A. Charlton, Nucl. Phys. A290, 128 (1977).
[13]J. D. Burch, M. J. Schneider, and J. J. Kraushaar, Nucl. Phys. A299, 117 (1978).
[14]R. N. Boyd, W. P. Alford, E. R. Flynn, and R. A. Hardekopf, Phys. Rev. C 15, 1160 (1977).
[15]J. C. Hardy, A. D. Bacher, G. R. Plattner, J. A. MacDonald, and R. G. Sextro, Phys. Rev. Lett. 25, 298 (1970).
[16]J. M. Nelson, N. S. Chant, and P. S. Fisher, Nucl. Phys. A156, 406 (1970).
[17]M. Pignarelli, I. Gosset, F. Resmini, B. Mayer, and J. L. Escudie, Phys. Rev. C 8, 2120 (1973).
[18]J. A. MacDonald, N. A. Jelley, and J. Cerny, Phys. Lett. 47B, 237 (1973).
[19]G. Igo, J. C. S. Chai, R. F. Casten, T. Udagawa, and T. Tamura, Nucl. Phys. A207, 289 (1973).
[20]E. R. Flynn, R. A. Hardekopf, J. D. Sherman, and J. W. Sunier, Phys. Lett. 61B, 433 (1976).
[21]K. Yagi, S. Kuneri, Y. Aoki, Y. Higashi, J. Sanada, and Y. Tagishi, Phys. Rev. Lett. 40, 161 (1978).
[22]R. A. Hardekopf, in *Proceedings of the Fourth International Symposium on Polarization Phenomena in Nuclear Reactions*, edited by W. Grüebler and V. König (Birkhauser, Basel, 1975), p. 865.
[23]G. G. Ohlsen, T. L. McKibben, G. P. Lawrence, P. W. Keaton, Jr., and D. D. Armstrong, Phys. Rev. Lett. 27, 599 (1971).
[24]W. P. Alford, R. A. Lindgren, D. Elmore, and R. N. Boyd, Nucl. Phys. A243, 269 (1975).
[25]E. R. Flynn, S. Orbesen, J. D. Sherman, J. W. Sunier, and R. Woods, Nucl. Inst. 128, 35 (1975).
[26]W. Darcey, R. Chapman, and S. Hinds, Nucl. Phys. A170, 253 (1971).
[27]F. D. Becchetti and G. W. Greenlees, Phys. Rev. 182, 1190 (1969).
[28]F. G. Perey, Phys. Rev. 131, 745 (1963).
[29]E. R. Flynn, D. D. Armstrong, J. G. Beery, and A. G. Blair, Phys. Rev. 182, 1113 (1969).
[30]P. D. Kunz, private communication.
[31]D. E. Rundquist, M. Brussel, and A. I. Yavin, Phys. Rev. 168, 1296 (1968).
[32]J. D. Childs, W. W. Daehnick, and M. J. Spisak, Phys. Rev. C 10, 217 (1974).
[33]S. Yoshida, Nucl. Phys. 33, 685 (1962).
[34]H. Nann, E. R. Flynn, D. L. Hanson, and S. Raman, Phys. Rev. C 18, 2511 (1978).
[35]L. S. Kisslinger and R. A. Sorenson, Matt. Fys. Medd. Dan. Vid. Selsk. 32 (1960), No. 9.
[36]R. H. Fulmer and A. L. McCarthy, Phys. Rev. 131, 2133 (1966).